J|A|C|S
ARTICLES
Published on Web 01/29/2004

Diffusion NMR Spectroscopy for the Characterization of the Size and Interactions of Colloidal Matter: The Case of Vesicles and Nanoparticles

Massimiliano Valentini,[†,‡] Andrea Vaccaro,[§] Annemie Rehor,[‡] Alessandro Napoli,[‡] Jeffrey A. Hubbell,[‡] and Nicola Tirelli*[,†,‡]

Contribution from the School of Pharmacy and Molecular Materials Centre, University of Manchester, Oxford Road, M13 9PL Manchester, United Kingdom, Institute for Biomedical Engineering and Department of Materials, Swiss Federal Institute of Technology (ETH) and University of Zurich, Moussonstrasse 18, CH-8044 Zurich, Switzerland, and Institute for Technical Chemistry, Swiss Federal Institute of Technology (ETH), ETH Hönggerberg, CH-8093 Zurich, Switzerland

Received July 13, 2003; E-mail: nicola.tirelli@man.ac.uk

Abstract: We report the application of the pulse gradient spin−echo (PGSE) NMR technique (PGSE NMR) to the analysis of large colloidal materials, specifically vesicles formed from macromolecular amphiphiles and nanoparticles. Measurements of size and size distribution were demonstrated to be comparable to those obtained through dynamic light scattering or hydrodynamic chromatography. In comparison to these more common analytical methods, the use of PGSE NMR is particularly advantageous in that, as a spectroscopic technique, it adds chemical selectivity to the study of physical dimensions. In this way, chemically different species contemporarily present in a sample may be individually studied. In addition, we demonstrate the use of PGSE NMR to probe the existence of equilibria between macroamphiphiles present in solution and those present in vesicles or on the surface of nanoparticles. This feature in particular opens exciting possibilities for the characterization of the phase behavior and of the surface adsorption phenomena of colloids.

Introduction

Typical analytical methods for colloidal materials focus on their dimensional characterization, as reflected by the predominance of static scattering methods, such as small-angle scattering of X-rays[1−5] or neutrons[1,6,7] and static light scattering,[8−11] and diffusive techniques, such as photon[2,12,13] and fluorescence correlation spectroscopy,[14,15] fluorescence recovery after photobleaching,[16−18] field-flow-fractionation,[19−21] and hydrodynamic chromatography.[21,22] Only a limited number of these techniques can provide insight into size distributions, and their results must be combined with spectroscopic analysis to yield information regarding materials composition. Virtually no method combines universal applicability to any material type with chemical selectivity to yield compositional analysis. Because of the ubiquity of colloidal materials in a wide variety of fields, such as drug delivery, polymerization processes, ceramic processing, and water and air analysis, to name only a few, the combination of universality with chemical sensitivity is particularly important, providing a strong motivation to develop approaches that exploit the power of NMR.

The application of the pulsed gradient spin−echo (PGSE) NMR technique[23,24] has recently opened some new possibilities

† University of Manchester.
‡ Institute for Biomedical Engineering and Department of Materials, Swiss Federal Institute of Technology and University of Zurich.
§ Institute for Technical Chemistry, Swiss Federal Institute of Technology.

(1) Pedersen, J. S.; Svaneborg, C. *Curr. Opin. Colloid Interface Sci.* **2002**, *7*, 158−166.
(2) Southon, P. D.; Bartlett, J. R.; Woolfrey, J. L.; Ben-Nissan, B. *Chem. Mater.* **2002**, *14*, 4313−4319.
(3) DiMasi, E.; Fossum, J. O.; Gog, T.; Venkataraman, C. *Phys. Rev. E* **2001**, *6406*, art. no.-061704.
(4) Boukari, H.; Long, G. G.; Harris, M. T. *J. Colloid Interface Sci.* **2000**, *229*, 129−139.
(5) Kerch, H. M.; Long, G. G.; Krueger, S.; Allen, A. J.; Gerhardt, R.; Cosandey, F. *J. Mater. Res.* **1999**, *14*, 1444−1454.
(6) Penfold, J. *Curr. Opin. Colloid Interface Sci.* **2002**, *7*, 139−147.
(7) Vrij, A. *Colloids Surf., A* **2003**, *213*, 117−129.
(8) Umbach, P.; Georgalis, Y.; Saenger, W. *J. Am. Chem. Soc.* **1998**, *120*, 2382−2390.
(9) Haraszti, T.; Dekany, I. *Colloid Polym. Sci.* **2002**, *280*, 736−743.
(10) Heimer, S.; Tezak, D. *Adv. Colloid Interface Sci.* **2002**, *98*, 1−23.
(11) Bushell, G. C.; Yan, Y. D.; Woodfield, D.; Raper, J.; Amal, R. *Adv. Colloid Interface Sci.* **2002**, *95*, 1−50.
(12) Buffle, J.; Leppard, G. G. *Environ. Sci. Technol.* **1995**, *29*, 2176−2184.
(13) Colfen, H.; Schnablegger, H.; Fischer, A.; Jentoft, F. C.; Weinberg, G.; Schlogl, R. *Langmuir* **2002**, *18*, 3500−3509.
(14) Akcakir, O.; Therrien, J.; Belomoin, G.; Barry, N.; Muller, J. D.; Gratton, E.; Nayfeh, M. *Appl. Phys. Lett.* **2000**, *76*, 1857−1859.
(15) Starchev, K.; Zhang, J. W.; Buffle, J. *J. Colloid Interface Sci.* **1998**, *203*, 189−196.
(16) Cheng, Y.; Prud'homme, R. K.; Thomas, J. L. *Macromolecules* **2002**, *35*, 8111−8121.
(17) Kluijtmans, S.; de Hoog, E. H. A.; Philipse, A. P. *J. Chem. Phys.* **1998**, *108*, 7469−7477.
(18) Imhof, A.; Dhont, J. K. G. *Phys. Rev. E* **1995**, *52*, 6344−6357.
(19) Colfen, H.; Antonietti, M. *New Developments in Polymer Analytics I*; Springer: New York, 2000; Vol. 150, pp 67−187.
(20) Thang, N. M.; Geckeis, H.; Kim, J. I.; Beck, H. P. *Colloids Surf., A* **2001**, *181*, 289−301.
(21) Janca, J.; Berneron, J. F.; Boutin, R. *J. Colloid Interface Sci.* **2003**, *260*, 317−323.
(22) Williams, A.; Varela, E.; Meehan, E.; Tribe, K. *Int. J. Pharm.* **2002**, *242*, 295−299.
(23) Price, W. S. *Concepts Magn. Reson.* **1997**, *9*, 299−336.

10.1021/ja037247r CCC: $27.50

Scheme 1

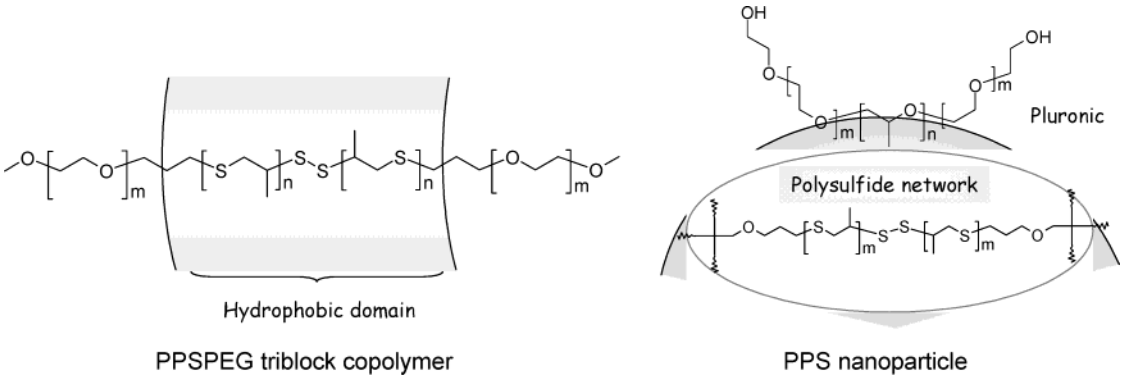

to analysis of materials, including colloids. This method allows the study of diffusional properties of objects in solution or dispersion through measurement of spectral characteristics, which are inherently chemically selective. When PGSE is applied to colloids, which generally feature a water- or solvent-exposed surface chemically different from a solid, gellike, or hydrophobic bulk, it is in principle possible to target the resonances of surface groups, thus at the same time performing a chemical and morphological selection.

The popularity of PGSE has been boosted by the development of 2D NMR diffusion ordered spectroscopy[25] (DOSY), a PGSE-based method that offers a good visual presentation of chemical shift data related to diffusion coefficients and, by the use of least-squares analysis or Laplace antitransform-based algorithms (e.g., CONTIN),[26,27] allows calculation of diffusion coefficient distributions from PGSE data.

Until now, the determination of the self-diffusion coefficients via PGSE NMR measurements has been successfully applied to a variety of systems: for example, to the characterization of size, composition, and association phenomena of substrates in solution, such as polymers,[28] organometallic complexes,[29] and other low MW compounds.[30] Size and aggregation processes, but also phase diagrams, have been investigated for small molecules in liquid crystals and porous solids,[31] and also for colloidal materials (micelles, supramolecular polymeric aggregates).[32,33]

Having in mind the advantages of the combination of a universal and chemically selective tool with size analysis, we sought to expand the application of PGSE NMR to larger colloidal particles, using it for the characterization of vesicles formed from macromolecular amphiphiles (polymersomes) and nanoparticles. Our group has recently developed such carrier structures for applications that include drug delivery, both being based on polyethers and polysulfides. The polyether component is based upon poly(ethylene glycol) (PEG), which is particularly interesting for display upon the colloid surface due to its favorable biocompatibility. The polysulfide component is based upon poly(propylene sulfide), which is interesting to us for its sensitivity to oxidation to a hydrophile, poly(propylene sulfone), under physiological conditions.[34] The vesicles are obtained from the triblock macroamphiphiles poly(ethylene glycol)-*bl*-(propylene sulfide)-*bl*-(ethylene glycol) (PEG-*bl*-PPS-*bl*-PEG copolymers),[35] the aqueous lamellar aggregates of which can be converted into polymersomes.[34,36] The nanoparticles are prepared via emulsion polymerization of propylene sulfide in water, using a poly(ethylene glycol)-*bl*-(propylene glycol)-*bl*-(ethylene glycol) (Pluronic F127) as an emulsifier.[37,38]

To the best of our knowledge, this report presents the first example of application of PGSE NMR to the study of polymersomes or nanoparticles, objects characterized by much larger dimensions than those of the colloidal materials studied until now. We demonstrate the utility of this technique not only for the characterization of the size and size distribution of the systems, but also for the study of surface reorganization phenomena, which are of paramount importance for determining the biocompatibility and the body clearance of drug carriers.

Experimental Section

Materials. D_2O was purchased from Cambridge Isotope Laboratories (Im Baumgarten, Switzerland) and used without further purification. Poly(ethylene glycol) with MW = 3400 (PEG 3400) was purchased from Fluka (Buchs, Switzerland) and used without further purification. Pluronic F127 was purchased from Sigma-Aldrich (Buchs, Switzerland) and used without further purification.

Preparation and Purification Procedures. The symmetric triblock copolymer poly(ethylene glycol)-*bl*-poly(propylene sulfide)-*bl*-poly(ethylene glycol) (PEG-*bl*-PPS-*bl*-PEG, $M_n \approx 5500$; Scheme 1, left), with 16 monomeric units for each PEG block and 50 for the PPS block, was synthesized as described elsewhere.[35] Polymersomes were prepared by soaking in D_2O (1% w/w), and then sonicating, films of PEG-*bl*-PPS-*bl*-PEG (produced by evaporation of dichloromethane solutions), as described elsewhere.[36] The resulting multilamellar, very large vesicles were then extruded with a Mini-Extruder (Avanti Lipids) with a 100 nm pore size polycarbonate membrane to reduce them to smaller, unilamellar polymersomes (structure shown in Scheme 1, left).

Nanoparticles were prepared in H_2O, by polymerizing propylene sulfide under dry nitrogen atmosphere using the triblock copolymer

(24) Price, W. S. *Concepts Magn. Reson.* **1998**, *10*, 197−237.
(25) Morris, K. F.; Johnson, C. S. *J. Am. Chem. Soc.* **1993**, *115*, 4291−4299.
(26) Provencher, S. W. *Comput. Phys. Commun.* **1982**, *27*, 229−242.
(27) Provencher, S. W. *Comput. Phys. Commun.* **1982**, *27*, 213−227.
(28) Jerschow, A.; Muller, N. *Macromolecules* **1998**, *31*, 6573−6578.
(29) Pichota, A.; Pregosin, P. S.; Valentini, M.; Worle, M.; Seebach, D. *Angew. Chem., Int. Ed.* **2000**, *39*, 153.
(30) Antalek, B. *Concepts Magn. Reson.* **2002**, *14*, 225−258.
(31) Callaghan, P. T.; Komlosh, M. E. *Magn. Reson. Chem.* **2002**, *40*, S15−S19.
(32) Griffiths, P. C.; Cheung, A. Y. F.; Davies, J. A.; Paul, A.; Tipples, C. N.; Winnington, A. L. *Magn. Reson. Chem.* **2002**, *40*, S40−S50.
(33) Holmberg, A.; Piculell, L.; Nyden, M. *J. Phys. Chem. B* **2002**, *106*, 2533−2544.
(34) Napoli, A.; Valentini, M.; Muller, M.; Tirelli, N.; Hubbell, J. A. *Nat. Mater.*, accepted.
(35) Napoli, A.; Tirelli, N.; Kilcher, G.; Hubbell, J. A. *Macromolecules* **2001**, *34*, 8913−8917.
(36) Napoli, A.; Tirelli, N.; Wehrli, E.; Hubbell, J. A. *Langmuir* **2002**, *18*, 8324−8329.
(37) Rehor, A.; Tirelli, N.; Hubbell, J. A. *Macromolecules* **2002**, *35*, 8688−8693.
(38) Rehor, A.; Tirelli, N.; Hubbell, J. A. *J. Controlled Release* **2003**, *87*, 246−247.

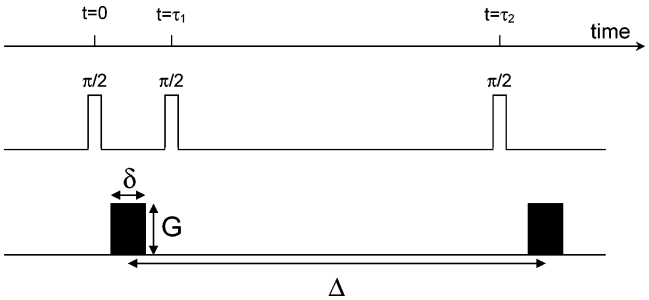

Figure 1. Stimulated-Echo sequence used in ^{1}H-PGSE NMR experiments. The black filled rectangles represent gradient pulses with length and amplitude equal to δ and to G, respectively. The diffusion time Δ is the interval between the midpoints of the gradients.

Pluronic F127 [poly(ethylene glycol)-*bl*-poly(propylene glycol)-*bl*-poly(ethylene glycol) (PEG-PPO-PEG), MW = 12 600, 70 wt % PEG], as an emulsifier, a tetrafunctional thiol as an initiator, and DBU as a base (0.025 g of Pluronic, 6.53 mmol of propylene sulfide, 0.128 mmol of initiator, 0.51 mmol of base), modifying a literature procedure based on the use of a difunctional initiator.[37] The polymer nanoparticles were then cross-linked by exposing them to air to induce disulfide bond formation, as described elsewhere (structure shown in Scheme 1, right).[38,39]

Some samples of both material families were purified by dialysis using polycarbonate membranes with different molecular weight cutoff (MWCO).

NMR Experiments. NMR measurements were performed on a Bruker AVANCE 500 MHz spectrometer equipped with a microprocessor-controlled gradient unit and a multinuclear probe with an actively shielded z-gradient coil. All samples were measured in the solvent used for the preparation, so that nanoparticles and dialyzed vesicles were measured in H_2O, while nonpurified vesicles were measured in D_2O. NMR tubes of 5 mm o.d. from Wilmad (507-PP) were used for these measurements.

The ^{1}H-PGSE NMR measurements were performed at 298 K without spinning and deuterium lock, using the three pulses Stimulated-Echo sequence[40,41] (Figure 1). A Bruker BBI (1H, 31P-103Rh) probe with actively shielded z-gradient was used in combination with a Bruker gradient amplifier board (GAB) providing a maximum current of 10 A, which results in a 56 G/cm gradient.

The minimum time required for eddy current effects to decay was found to be around 200 μs, so that delays between the first $\pi/2$ pulse and the first gradient and between the last gradient and the acquisition were set equal to 1 ms. The shapes of the gradients were rectangular, and their lengths (δ) were varied automatically in the course of the experiments in the range 0.1−15.0 ms, leaving all of the remaining parameters unchanged. The diffusion time, Δ, was held constant so that the attenuation resulting from spin−lattice relaxation (T_1) would not vary, and typically Δ values were in the range 50−150 ms. Gradient strengths between 0.35 and 0.50 T m^{-1} were used. The measurements were performed with the deuterium lock turned off, to avoid field-frequency drift or oscillation during the experiment caused by spectrometer lock disturbances from the field gradient pulses.

For a single diffusing species, the free induction decay (FID) amplitude is given by eq 1,

$$A(\tau_1 + \tau_2) = \frac{A(0)}{2} \exp\left[-\frac{\tau_2 - \tau_1}{T_1} - \frac{2\tau_1}{T_2} - (\gamma G\delta)^2 D\left(\Delta - \frac{\delta}{3}\right)\right] \quad (1)$$

where $A(\tau_1 + \tau_2)$ and $A(0)/2$ are the amplitudes of the echo with and without gradients, respectively, T_1 and T_2 are the longitudinal and transverse relaxation times, respectively, D is the diffusion coefficient of the species under investigation, γ is its gyromagnetic ratio, and the other parameters are as defined in Figure 1. For nuclei having relatively long relaxation times, determined by standard inversion recovery for T_1 and a CPMG-based sequence for T_2,[42] eq 1 can be rewritten as

$$A(\tau_1 + \tau_2) = \frac{A(0)}{2} \exp\left[-(\gamma G\delta)^2 D\left(\Delta - \frac{\delta}{3}\right)\right] \quad (2)$$

After Fourier transformation, the echo amplitudes are proportional to the signals' intensities, and one obtains:

$$\ln\left(\frac{I}{I_0}\right) = -(\gamma G\delta)^2 D\left(\Delta - \frac{\delta}{3}\right) = -kD \quad (3)$$

where I and I_0 are the intensities of the NMR peaks with and without the gradients. The diffusion coefficient D is generally determined as the slope of the linear plot of $\ln(I/I_0)$ versus k, where k is equal to $(\gamma G\delta)^2(\Delta - \delta/3)$. Through the Stokes−Einstein equation (eq 4), it is finally possible to correlate the diffusion coefficient with its hydrodynamic radius r_H:

$$r_H = \frac{k_B T}{6\pi\eta D} \quad (4)$$

where k_B is the Boltzmann constant, T is the temperature expressed in Kelvin, and η is the viscosity of the solution.

Data Treatment. In the most general case of a polydisperse sample, the diffusion coefficient distribution is related to the intensities of the NMR peaks through the following relationship:

$$\frac{I}{I_0} = \int_0^\infty P(D) \exp(-kD)\, dD \quad (5)$$

which is obtained from eq 3 assuming NMR intensity additivity ($P(D)$ being the distribution function of D). In this mathematical treatment, analogous to that applied to dynamic light scattering data, eq 5 presents the problem of a physically interesting function, such as the diffusion coefficient distribution, which is to be obtained from noisy experimental data through the numerical inversion of an integral equation. In the most common approach to this problem, a priori information about the unknown distribution is applied to the experimental data. The most common such regularization adopted is that due to Tikhonov,[43] which, among the distributions fitting the experimental data, favors the smoothest. In this work, the inversion of eq 5 was performed using CONTIN:[26,27] a Fortran IV software package that implements a Tikhonov regularization coupled with nonnegativity constraints in the framework of least-squares programming. This approach has provided a good agreement with the results of other experimental techniques; however, several other approaches can also be used, such as CORE analysis, provided there is previous knowledge of some parameters of the distribution.[44]

Other Physicochemical Characterization. Hydrodynamic chromatography was performed using a PL-PSDA hydrodynamic chromatography apparatus (Polymer Laboratories) calibrated with polystyrene latex standards. Dynamic light scattering was performed using a BI-200SM goniometer (Brookhaven) and an argon-ion laser M95-2 (Lexel) at a scattering angle of 90°, using Milli-Q (Millipore) deionized water for sample dilution, polystyrene latex standards as references, and a CONTIN algorithm for data inversion.

Results and Discussion

Nature of the Colloidal Species. The polymersomes used in the present work are colloidal objects in which a water cavity

(39) Rehor, A.; Tirelli, N.; Hubbell, J. A., manuscript in preparation.
(40) Tanner, J. E. *J. Chem. Phys.* **1970**, *52*, 2523.
(41) Stilbs, P. *Prog. Nucl. Magn. Reson. Spectrosc.* **1987**, *19*, 1−45.
(42) Claridge, T. D. W. *High-Resolution NMR Techniques in Organic Chemistry*; Elsevier Science: Oxford, 1999.
(43) Groetsch, C. W. *The theory of Tikhonov regularization for Fredholm equations of the first kind*; Pitman: Boston, 1984.
(44) Stilbs, P. *J. Magn. Reson.* **1998**, *135*, 236−241.

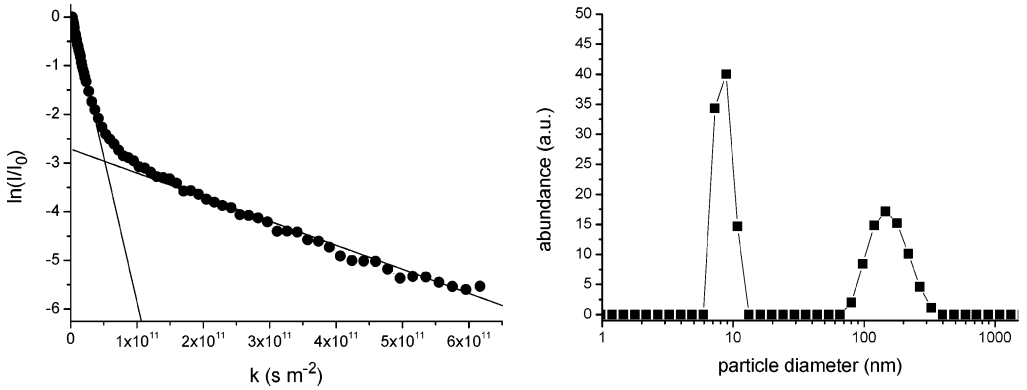

Figure 2. Left: Plot of the PEG-echo attenuation, $\ln(I/I_0)$ versus k, $k = (\gamma\Delta\delta)^2(\Delta - \delta/3)$ for "as-synthesized" nanoparticles in 1 wt % water dispersion. Right: Semilog plot of the size distribution of PEG-containing objects in the same sample, obtained from PGSE data after inversion with CONTIN. The log scale does not allow visual comparison of the relative quantities of the two components; in a linear scale, the micelle-associated peak is about 20 times smaller (because it is much narrower) than the nanoparticle-associated peak.

is surrounded by few nanometer-thick membrane of PEG-*bl*-PPS-*bl*-PEG;[36] polysulfide nanoparticles feature on the contrary a bulk composed of PPS and a surface displaying a PEG-containing emulsifier (Pluronic F127) physically adsorbed during the episulfide polymerization. The different natures of their bulk characteristics make them complementary for the kind of the molecules that can be hosted within (and eventually released): hydrophilic for the vesicles and hydrophobic for the nanoparticles. Despite the morphological differences and a completely different preparation procedure, they share several structural features. First, a PEGylated surface dominates both colloidal systems. In the case of the polymersomes, PEG is an integral part of the only molecular constituent, the macroamphiphile, and in the case of the nanoparticles, PEG is present as the hydrophilic component of the surface-adsorbed emulsifier. In both cases, PEG is exposed to water, is responsible of the particle stability toward aggregation, and displays in the ^{1}H NMR a sharp, intense signal similar to that of free PEG in solution.[45] Second, PPS is present as the hydrophobic component of both systems. This polymer was chosen for its responsiveness to oxidation (it can be oxidized to the more hydrophilic polysulfoxide or polysulfone[34] and thus induce destabilization of the structure) and its low glass transition temperature. Its ^{1}H NMR spectrum shows very broad, featureless signals, due to the short relaxation times typical of nuclei in hydrophobic domains. Due to the sharpness and intensity of the ethylene glycol signal, we decided to perform PGSE experiments monitoring its resonance, thus focusing our attention on surface groups.

Nanoparticles. Polysulfide nanoparticles are obtained from emulsion polymerization and then dialyzed to remove residual monomer. A relevant issue for their use as carriers is whether their water dispersions may contain also other colloidal species, which may alter the loading and release profile for guest molecules.

PGSE experiments show two linear regimes in the plot of $\ln(I/I_0)$ (echo attenuation) versus k, suggesting the contemporary presence of two PEG-containing species with markedly different diffusion coefficients: 6.2×10^{-11} and 4.3×10^{-12} m^2 s^{-1}, corresponding to hydrodynamic radii of ca. 3 and 60 nm, respectively (Figure 2, left). The smaller-sized component shows

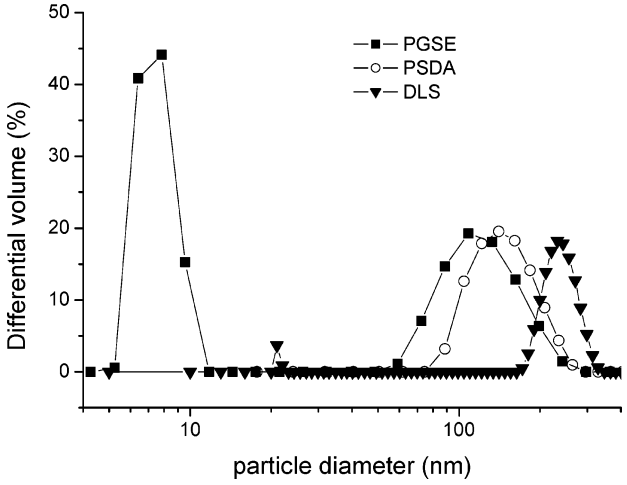

Figure 3. Comparison of the size distribution plots obtained with ^{1}H-PGSE NMR, hydrodynamic chromatography (PSDA), and dynamic light scattering (DLS) for PPS nanoparticles in a 1 wt % water dispersion.

the same diffusion coefficient as reported for free Pluronic F127 dispersed in water, which, at room temperature and low concentration, exists in a micellar state.[46] On the other hand, nanoparticles constitute the larger component. The application of the Laplace inverse transform correspondingly provides a bimodal size distribution (Figure 2, right), which, integrated, reveals the presumptive micellar component to constitute ~5.5% of the total Pluronic content. The same result can be obtained by separately fitting the two linear components of the graph in Figure 2, left, and comparing their intercepts (at $k = 0$).

The size distribution provided by hydrodynamic chromatography (PSDA) substantially confirmed the average size of the nanoparticles, with diameters of 120 nm measured by PGSE versus 140 nm by PSDA, but this technique is completely insensitive to the smaller-sized component (Figure 3). On the other hand, the comparison of PGSE measurements with characterization by dynamic light scattering (DLS), shown in Figure 3, revealed not only that micelles were neglected by DLS, but also that the method considerably overestimated the size of the nanoparticles. However, the three techniques provided similar results for the polydispersity of the nanoparticle distribution.

(45) Valentini, M.; Napoli, A.; Tirelli, N.; Hubbell, J. A. *Langmuir* **2003**, *19*, 4852−4855.

(46) Linse, P. *Macromolecules* **1993**, *26*, 4437−4449.

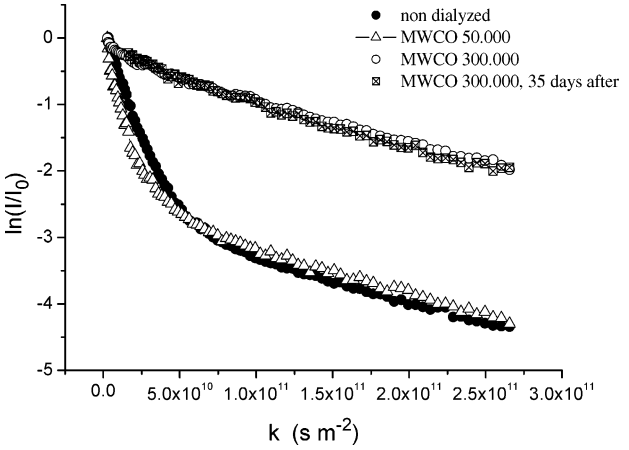

Figure 4. Echo attenuation plots of nanoparticles before dialysis, after dialysis with medium pore membranes (50 000 MWCO), and after dialysis with large pore membranes (300 000 MWCO) for 7 d and further after 35 d of reequilibration in distilled water. The loss of the smaller-sized component is evident with an increase in the MWCO of the dialysis membranes. Recovery of the micelle-associated signal is not observed after 35 d, indicating the absence of rapid equilibration between surface-bound and free Pluronic.

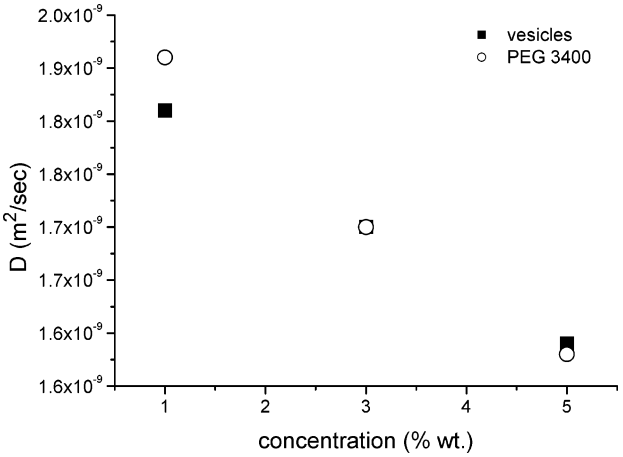

Figure 5. Concentration dependence of the diffusion coefficients of water for PEG3400 and PEG-*bl*-PPS-*bl*-PEG vesicles 1, 3, and 5 wt %.

The reason of this poor sensitivity of DLS and PSDA is likely ascribed to two factors: the small difference in refractive index between Pluronics and water (as opposed to the one between polysulfide and water) and the very low concentration of the small-sized component, which accounts for roughly the 0.015% of the total polymer mass. One has indeed to stress that PGSE compares just the surface components, while DLS and PSDA compare the total volumes of the objects.

The free Pluronic that was observed to exist as micelles within the nanoparticle suspension could remain from the polymerization process (that fraction could have not participated in stabilization of the emulsion prior to and during polymerization) or could be present due to desorption after polymerization in an equilibrium process. We have discriminated between these two hypotheses by removing the free polymer and allowing the system to reequilibrate. Using dialysis membranes with an appropriate molecular weight cutoff (MWCO = 300 000), the nanoparticles were separated by the free polymer, simplifying the $\ln(I/I_0)$ versus k plot to a single linear trace and the resulting PGSE size distribution to a monomodal curve (Figure 4). The micellar component was not recovered by storing the particles in distilled water or in buffered saline for periods up to 35 d. Thus, the desorption of Pluronic from the nanoparticle surface appears to be a very slow process, if happening at all, and it would seem that the equilibrium was reached before polymerization, from the surface of the colloidal dispersion of liquid propylene sulfide. It may be that the Pluronic is actually entangled with the PPS at the particle surface, the entanglement resulting from penetration of the poly(propylene glycol) component of the Pluronic into the propylene sulfide nanodroplet, with stable entanglement resulting from a semi-interpenetrating network at the colloidal particle surface.

Polymersome Vesicles. While the application of PGSE to nanoparticles was unprecedented, studies on vesicles have been reported.[47] In these studies, the self-diffusion coefficient of water was used for characterizing liposome suspensions: in the presence of the liposomes, the value of D_{H_2O} decreases due to obstructions induced by the colloidal particles and hydration of the polar headgroups of the liposome surfactants. From these measurements, it is thus possible to estimate the amount of water entrapped within the vesicles and hence the size of the aggregates.

In the presence of PEG-*bl*-PPS-*bl*-PEG polymersomes, we indeed observed an attenuation of the water self-diffusion coefficient. The linear character of the plots showed that the experiments were unable to distinguish between two populations of water molecules (inside and outside the polymersomes), suggesting a high permeability of water through the membrane (Figure 5). However, once we applied the model reported by Olsson[48] for fast exchange conditions, the calculations produced unrealistically low dimensions (around 5 nm in diameter, roughly the size of an isolated PEG-*bl*-PPS-*bl*-PEG molecule). This result cannot be explained by a possible lack of sensitivity, due to a too little quantity of encapsulated water. The same value of diffusion coefficient was obtained for vesicular dispersions at 1, 3, and 5 wt %, which contain nonnegligible water quantities: assuming an average size of 100 nm and a membrane thickness of 8 nm (as estimated from cryo-TEM measurements[34]), the amount of encapsulated water is respectively 1.5%, 4.5%, and 7.5% of the total water volume. Furthermore, the behavior of the water self-diffusion coefficients in the presence of polymersomes was indistinguishable from that recorded in the presence of PEG 3400 in the same concentration range (Figure 5). This polymer does not aggregate in water, and the decrease in D is imputable mostly to the increase in viscosity in the medium and to the number of water molecules structured around the polymer chain. Thus, water molecules seem not to feel PEG-*bl*-PPS-*bl*-PEG in water as an aggregated and impermeable system. The PGSE characterization suggests that the PPS domain of the membrane does not substantially resist water transport.

Because the application of previously employed methods for characterization of the vesicles was not possible for the PEG-*bl*-PPS-*bl*-PEG polymersomes, we employed the same approach as we did for nanoparticles, monitoring the echo attenuation of

(47) Caria, A.; Regev, O.; Khan, A. *J. Colloid Interface Sci.* **1998**, *200*, 19−30.

(48) Olsson, U.; Nakamura, K.; Kunieda, H.; Strey, R. *Langmuir* **1996**, *12*, 3045−3054.

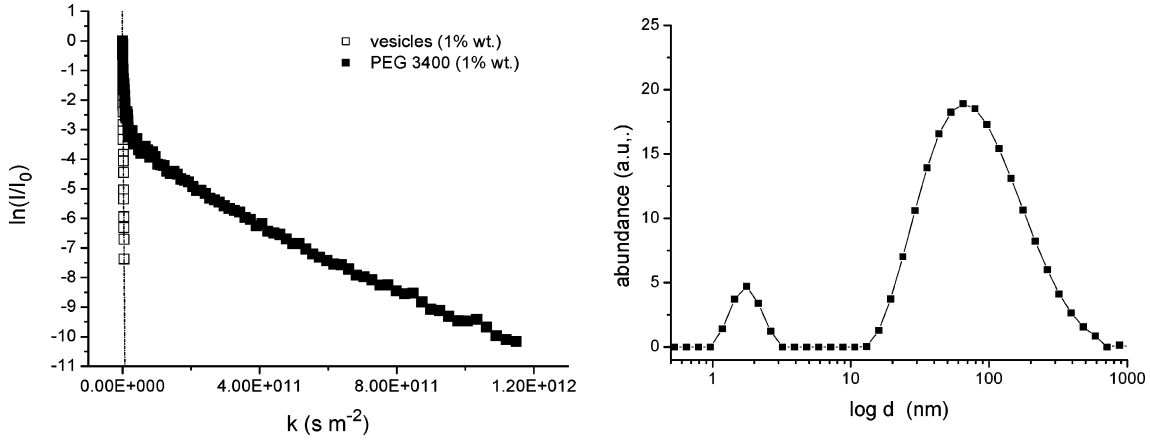

Figure 6. Left: Echo attenuation plots of a 1 wt % PEG-*bl*-PPS-*bl*-PEG vesicle suspension (as extruded) as compared to a 1 wt % PEG 3400 water solution. The steep part of the curve recorded for vesicles overlaps well with that of the soluble polymer, indicating a similar diffusion coefficient. Right: Size distribution of the vesicle suspension obtained from PGSE measurements after inversion with CONTIN.

the PEG resonance, with successful results. The lamellar aggregates formed by hydration of PEG-*bl*-PPS-*bl*-PEG block copolymer films are converted into vesicular assemblies via sonication and extrusion through porous membranes. In this case, DLS and PGSE analysis provided similar results.

As was the case in our characterization of the nanoparticles, it was necessary to determine if other colloidal species are formed in this process, to determine if they exist in equilibrium with the vesicles, and finally to qualify a purification procedure.

As shown in Figure 6, a smaller-sized component (3−5 nm in diameter, roughly 3% of the total polymer content) was observed in the dispersion along with larger polymersomes after extrusion. This component has a diffusion coefficient similar to that of a PEG of similar molecular weight (MW = 3400); we therefore believe it to be composed of individual PEG-*bl*-PPS-*bl*-PEG molecules, which, due to their fairly low CMC (10^{-5}−10^{-7} M, corresponding to at most 0.005 wt %[49]), are most likely in the state of monomolecular micelles. Dialysis effectively separated the larger colloidal objects from smaller micelles. Also, in this case, the micellar component was not restored upon storage.

The PEG-*bl*-PPS-*bl*-PEG copolymers used in this research form stable lamellar phases at room temperature in water; thus, with this composition and MW, structures with higher curvature, such as micelles, need some excess energy to be formed. This hypothesis is confirmed by the absence of spontaneous generation of micelles upon storage. On the other hand, the mechanical energy provided during extrusion is likely responsible for the presence of micelles after this process. These micelles coexist with vesicles and are not in (quick) equilibrium with them. The absence of a reequilibration to a lamellar state is most probably due to the high energetic barrier arising from repulsion of the PEG layer: migration of single molecules or fusion of the aggregates is indeed an unlikely phenomenon, as it is also demonstrated that vesicles do not fuse for giving an optimal "equilibrium" size that minimizes the curvature energy. The polymersomes are therefore to be thought of as kinetically trapped structures.

(49) Napoli, A., unpublished results.

Conclusions

We have applied ^{1}H-PGSE for characterization of nanoparticles and vesicles formed from polymeric amphiphiles. Targeting surface groups of these colloidal objects, we demonstrated that ^{1}H-PGSE can provide accurate size distributions, both in purified systems as well as in the presence of other colloidal components, such as micelles.

We also showed that ^{1}H-PGSE can be used for studying surface equilibria. The PEGylated emulsifier (Pluronic) was irreversibly adsorbed or entangled upon the surface of the PPS nanoparticles. This ensures a stable, nonrestructuring coverage of the particle by a "stealth" polymer, a promising phenomenon for applications in body fluids. We also demonstrated that PEG-*bl*-PPS-*bl*-PEG in polymersome vesicles is not in rapid equilibrium with the micelles produced in the process of vesicle formation. This is a key requirement, having in mind the use of these polymersomes as drug carriers: morphological stability is in fact of the essence for avoiding phase transitions and the consequent uncontrolled release of encapsulated material upon dilution of the polymersome dispersion by injection in the body.

Thus, in the two examples presented, we demonstrate the flexibility of ^{1}H-PGSE in the analysis of large colloidal objects, detecting the presence of different populations of objects with the same surface chemistry (chemically selective size analysis), determining the efficiency of purification methods (quality control analysis), and finally assessing the presence or absence of equilibria on time scales of interest (study of the colloidal dynamics).

Acknowledgment. The authors gratefully acknowledge Dr. Heinz Ruegg (Department of Chemistry, ETH Zurich) for helpful discussions. The authors are also indebted to Gebert Rüf Stiftung (Basel, Switzerland) for the fundamental financial contribution.

Supporting Information Available: Plots of experimental data (PDF). This material is available free of charge via the Internet at http://pubs.acs.org.

JA037247R